A theory of vibrational energy relaxation in liquids

Cite as: J. Chem. Phys. **105**, 7047 (1996); https://doi.org/10.1063/1.472506
Submitted: 20 May 1996 . Accepted: 15 July 1996 . Published Online: 04 June 1998

S. A. Egorov, and J. L. Skinner

A theory of vibrational energy relaxation in liquids

S. A. Egorov and J. L. Skinner
Theoretical Chemistry Institute and Department of Chemistry, University of Wisconsin, Madison, Wisconsin 53706

(Received 20 May 1996; accepted 15 July 1996)

A microscopic statistical mechanical theory of the vibrational energy relaxation of a diatomic solute in an atomic solvent is presented. The diatomic is treated as a breathing Lennard-Jones sphere. The relaxation rate is obtained from the Fourier transform of the force–force time-correlation function. The latter is expanded in powers of time (up to t^4), and expressions for the expansion coefficients are derived using equilibrium statistical mechanics. These coefficients are used to determine the parameters of an analytic ansatz for this correlation function, which can be evaluated at all times (and thus can be Fourier transformed). The resulting theory for the time-correlation function is compared to numerical results from a molecular dynamics simulation. Theoretical results for the vibrational relaxation rate are compared to experiments on I_2 in Xe over a wide range of densities and temperatures. © *1996 American Institute of Physics.* [S0021-9606(96)02339-2]

I. INTRODUCTION

The problem of vibrational energy relaxation is of central importance for understanding chemical dynamics in solution because reaction pathways are dictated by energy transfer rates in and out of vibrational modes. As such, many experimental studies of vibrational energy relaxation (VER) have appeared,[1–21] and several detailed reviews on the subject are available.[22–30] These experimental studies of VER rates are carried out in the time domain using pulsed laser techniques. Measured relaxation times range from picoseconds to seconds.[28]

The theoretical description of VER processes can be quite complicated, as the relaxation of a polyatomic solute in a polyatomic solvent can involve intramolecular pathways, intermolecular vibration–vibration (excitonic) energy transfer, and vibration–translation and vibration–rotation energy transfer. The simplest situation involves a diatomic solute at infinite dilution in an atomic solvent, in which case the vibrational energy of the solute can only be transferred into the solute's rotation and into translational degrees of freedom. This last mechanism of vibration–translation energy transfer might be considered the most fundamental one, since it dominates relaxation for simple systems and still plays an important role in even the most complicated situations. As such, vibration–translation energy transfer has been studied theoretically with several approaches. Of particular interest is the dependence of the VER rate on the vibrational frequency of the solute, the density and temperature of the solvent, and on the form of the intermolecular potentials.

One of the earliest theoretical approaches to VER in liquids involves the isolated binary collision model.[5,31–38] In this approach the VER rate is given by a product of two factors: The collision frequency, and the probability per collision that a transition will take place. The former depends on both the density and temperature of the liquid, while the latter is assumed to be a purely binary property, and therefore, depends only on the temperature. In earlier works the collision frequency was estimated from cell models,[32] while in more recent studies it was related to pair distribution functions.[5,31] The relaxation probability per collision can be obtained from scattering calculations.[38,39] The appropriateness of using the isolated binary collision model to calculate VER rates in liquids has been questioned.[33,34,40]

Another theoretical approach to VER involves the use of classical molecular dynamics computer simulation.[41–44] This method has the advantage that if the temperature is high enough to render the motion classical, for a given potential surface one obtains the exact answer, to arbitrary accuracy. Its principal liability is that for many systems at room temperature and below, vibrations are not classical. In addition, it is difficult to determine the dependence of VER rates on system variables since each choice can require a lengthy simulation.

Most recent theoretical work[40,42–62] on vibration–translation energy relaxation processes in liquids is based on time-dependent perturbation theory in the form of Fermi's Golden Rule. Quite generally, one can partition the Hamiltonian into a subsystem involving the solute's vibrational mode, a subsystem involving all the translation degrees of freedom (the bath), and the interaction between them. If the coupling between the vibration and the bath is sufficiently weak, second-order perturbation theory can be used to calculate the transition rate between the solute's vibrational (quantum) states. One finds that the overall VER rate is proportional to the Fourier transform (at the oscillator's frequency) of the ''force-force'' time correlation function (TCF). In this case the force is that felt by the solute's vibration due to the interaction with the solvent. In principle, this TCF should be evaluated quantum mechanically. In practice, however, it is usually the case that translations can be treated classically (even if the vibration cannot), and so this correlation function can be evaluated classically. This leads to what is usually called the Landau–Teller formula.[28]

There have evolved several approaches for calculating the appropriate force-force TCF required by the above formalism. One such approach treats the solvent as a hydrodynamic continuum,[49–51] which has its obvious limitations, at

least in terms of providing a molecular interpretation. Another involves the use of classical molecular dynamics simulation.[42–45,52,53] Very recently it has been suggested that ''instantaneous normal modes,'' usually obtained from a computer simulation, can also be used to calculate this correlation function.[54–56] Langevin equation simulation approaches, where the solvent is not treated explicitly, have also been invoked.[57–59] The primary difficulty associated with these three simulation approaches is that for high-frequency vibrations the Fourier transform of the TCF is extremely sensitive to any statistical noise in the correlation function itself.

Analytic statistical mechanical (molecular) theories of the force–force TCF are scarce. Indeed, accurate calculations of time correlation functions in liquids for all times is extremely difficult. (For recent attempts see references[63,64]). However, within the framework discussed above, what is needed is the Fourier transform of the TCF at the oscillator's frequency. If this frequency is sufficiently high, the Fourier transform will depend most sensitively on the short-time dynamics of the TCF. This suggests that a short-time expansion of the TCF, together with an appropriate ansatz for extrapolating the TCF to long times, might be successful. The power of this approach is that the short-time expansion coefficients can be obtained from *equilibrium* statistical mechanics.[65]

Adelman *et al.*[60–62] have taken essentially this approach. They calculate the first two nonvanishing terms in the short-time expansion of the TCF (i.e., its zero-time value and the coefficient of the t^2 term), and then assume that its full time dependence is given by a Gaussian, the normalization and width of which are chosen so that it is consistent with these two coefficients. Because the coefficient of the t^2 term is correct, this ansatz correctly describes the inertial behavior of the TCF, but it necessarily introduces errors in the higher-order terms in the series expansion. Since the fastest change of the TCF, and hence the region most crucial for its high-frequency Fourier transform, typically occurs in the region where the inertial approximation ceases to be valid, the Gaussian ansatz is not expected to be accurate for high frequencies.

In this paper, we develop a microscopic statistical mechanical theory of VER in liquids that is based on the short-time expansion of the TCF described above, but which goes beyond the Gaussian ansatz. Our theory is designed to apply to the case of diatomic molecules at infinite dilution in an atomic solvent. In this first version of the theory (the present paper), in order to avoid the difficulties associated with angle-dependent potentials, we assume that the diatomic molecule interacts with the solvent with a spherically symmetric potential, and that its vibrational coordinate also has spherical symmetry. Such a ''breathing sphere'' model has been considered elsewhere.[52,66] With this model we are able to calculate the first *three* nonvanishing terms in the short-time expansion of the TCF. We then use an ansatz originally suggested for a different problem by Douglass[67] and expanded upon by Isbister and McQuarrie[68] to model the TCF for all times. One can Fourier transform this ansatz analytically, which leads to an expression for the VER rate in terms of the short-time expansion coefficients. We derive formulas for the latter using equilibrium statistical mechanics. As such, they depend on the solute–solvent and solvent–solvent radial distribution functions. These are obtained using the hybrid mean spherical approximation (HMSA) integral equation technique,[69] which we have shown to be exceedingly accurate for dilute Lennard-Jones solutions.[70]

The organization of this paper is as follows. In Sec. II we discuss the model Hamiltonian and sketch the usual derivation of the TCF expression for the relaxation rate. In Sec. III we derive our expressions for the short-time expansion coefficients of the TCF, and discuss the ansatz for the full time dependence of the TCF and the resulting analytic expression for the relaxation rate. In Sec. IV we compare our theory for the TCF with exact results from molecular dynamics simulation. In Sec. V we compare our theoretical results for the relaxation rate with experiments[13] on I_2 in Xe for a wide range of solvent densities and temperatures; we find reasonably good agreement between theory and experiment, with one adjustable parameter. In Sec. VI we conclude.

II. MODEL HAMILTONIAN AND TCF EXPRESSION FOR THE VER RATE

As discussed above, we consider a single diatomic solute immersed in a monatomic fluid. We assume that the diatomic interacts with the solvent atoms with a spherically symmetric pair potential, and in addition, that the diatomic's vibrational coordinate has spherical symmetry. The solvent atoms also interact in a pairwise fashion. Therefore, the total (quantum-mechanical) Hamiltonian is

$$H = H_q + T + U, \tag{1}$$

where

$$H_q = \frac{p^2}{2m} + \frac{m\omega^2 q^2}{2}, \tag{2}$$

$$T = \frac{p_0^2}{2m_0} + \sum_i \frac{p_i^2}{2m_s}, \tag{3}$$

$$U = \sum_i \phi(r_{i0}, q) + \sum_{i<j} \phi_s(r_{ij}). \tag{4}$$

In the above H_q is the (harmonic) Hamiltonian associated with the solute's vibrational coordinate, q, whose conjugate momentum is p, reduced mass is m, and angular frequency is ω. T is the total translational kinetic energy of the solute and solvent atoms. The solute has momentum $\vec{p}_0$ and mass m_0, the summation indices refer to solvent atoms and go from one to N, and the ith solvent atom has momentum $\vec{p}_i$ and mass m_s. U is the total interparticle potential energy. $\phi(r,q)$ is the (q-dependent) solute–solvent pair potential, and r_{i0} is the distance between the ith solvent atom and the diatomic. $\phi_s(r)$ is the solvent–solvent pair potential, and r_{ij} is the distance between the ith and jth solvent atoms.

In order to isolate the perturbation that couples the diatomic vibrational mode to the translational degrees of freedom, we expand the solute–solvent pair potential to first order in q

$$\phi(r,q) \simeq \phi(r,0) + q \left. \frac{\partial \phi(r,q)}{\partial q} \right|_{q=0}. \tag{5}$$

Defining $\phi(r) = \phi(r,0)$ and $f(r) = -(\partial \phi(r,q)/\partial q)|_{q=0}$, the total Hamiltonian can now be written as

$$H = H_q + H_0 + V, \tag{6}$$

where

$$H_0 = T + U_0, \tag{7}$$

$$U_0 = \sum_i \phi(r_{i0}) + \sum_{i<j} \phi_s(r_{ij}), \tag{8}$$

$$V = -qF, \tag{9}$$

$$F = \sum_i f(r_{i0}). \tag{10}$$

Thus, H_0 is the Hamiltonian for the translational degrees of freedom, and its potential energy U_0 involves the solute–solvent pair potential $\phi(r)$, which is independent of q. V is the perturbation coupling the vibration to the bath, and F is therefore the force of the solvent acting on the vibrational coordinate.

Lowest-order perturbation theory gives the following result[22] for the transition rates between the eigenstates of H_q (the solute's vibrational states), which are labeled by n and have energy E_n

$$k_{n \to n'} = \frac{1}{\hbar^2} \int_{-\infty}^{\infty} dt \, \exp(i\omega_{nn'}t) \langle V_{nn'}(t) V_{n'n}(0) \rangle. \tag{11}$$

$\omega_{nn'} = (E_n - E_{n'})/\hbar$, $V_{nn'}(t)$ is the nn' matrix element of the time-dependent perturbation $V(t) = e^{iH_0 t/\hbar} V e^{-iH_0 t/\hbar}$, and $\langle \cdots \rangle$ indicates a trace over bath quantum states weighted by the equilibrium density operator for the bath. Since H_q is harmonic the transition rates are nonzero only if n and n' differ by one, and, for example,

$$k_{n \to n-1} = \frac{n}{2m\hbar\omega} \int_{-\infty}^{\infty} dt \, \exp(i\omega t) \langle F(t) F(0) \rangle, \tag{12}$$

where $F(t) = e^{iH_0 t/\hbar} F e^{-iH_0 t/\hbar}$. Thus we see that this result involves a quantum-mechanical force–force TCF.

The force–force TCF involves a bath operator F, propagated in time with the bath Hamiltonian, H_0. It is extremely difficult to evaluate. In fact, since $\hbar$ times the angular ''frequencies'' of the bath modes are typically less than kT, a common approximation is to treat the translational motion classically. However, a direct classical approximation to this TCF is unsatisfactory, because it would give equal rates for upward and downward transitions, in contradiction with the detailed balance condition. To avoid this difficulty, one can rewrite the quantum result in terms of a time-symmetrized anticommutator[22]

$$k_{n \to n-1} = \frac{2n}{m\hbar\omega[1 + \exp(-\beta\hbar\omega)]} \int_0^{\infty} dt \, \cos(\omega t) \times (1/2) \langle [F(t), F(0)]_+ \rangle, \tag{13}$$

where $\beta = 1/kT$. This symmetrized quantum TCF is a real, even function of time. These properties are also characteristic of a classical TCF. Thus, Eq. (13) is a convenient place to replace the symmetrized quantum TCF by its classical analogue, since in this way the detailed balance condition will still be satisfied. Therefore, we have

$$k_{n \to n-1} \simeq \frac{2n}{m\hbar\omega[1 + \exp(-\beta\hbar\omega)]} \int_0^{\infty} dt \, \cos(\omega t) \times \langle F(t) F(0) \rangle, \tag{14}$$

where now the angular brackets denote a classical equilibrium average, and $F(t)$ is simply the time-dependent classical force. We can define a modified classical TCF by

$$C(t) = \langle F(t) F(0) \rangle - \langle F \rangle^2, \tag{15}$$

which has the nice property that it vanishes as t becomes infinite. For finite ω one can just as well express the transition rate in terms of $C(t)$

$$k_{n \to n-1} = \frac{2n}{m\hbar\omega[1 + \exp(-\beta\hbar\omega)]} \int_0^{\infty} dt \, \cos(\omega t) C(t). \tag{16}$$

In some experiments the first excited vibrational state is populated initially. If one is in the low-temperature limit ($kT \ll \hbar\omega$), then the subsequent time evolution of the excited state population is described approximately by exponential relaxation to the ground state, with a rate constant $k_{1 \to 0}$. For other initial conditions and/or at higher temperatures, however, one has to deal with the whole vibrational manifold, and the associated set of rate constants. Nevertheless, for a harmonic oscillator coupled linearly (in the oscillator coordinate) to a bath, as above, energy relaxation can still be described by a single parameter—the relaxation time T_1 defined by the equation[71,72]

$$\frac{d\overline{E(t)}}{dt} = -\frac{1}{T_1} [\overline{E(t)} - E_{eq}], \tag{17}$$

where $\overline{E(t)}$ is the (nonequilibrium) average oscillator energy at time t, and E_{eq} is the average energy in thermal equilibrium. To obtain this result,[72] one writes the average energy in terms of the oscillator eigenvalues and the nonequilibrium diagonal density matrix elements: $E(t) = \Sigma_n \rho_{nn}(t) E_n$. The time evolution of the diagonal density matrix elements is given by the usual master equation. Using the above expressions for the relaxation rate constants one arrives at Eq. (17), and T_1 is given by

$$\frac{1}{T_1} = \frac{2 \tanh(\beta\hbar\omega/2)}{\hbar\omega m} \int_0^{\infty} dt \, \cos(\omega t) C(t). \tag{18}$$

Thus, to obtain T_1, one needs to calculate the classical force–force TCF, and to take its Fourier transform at the oscillator frequency ω.

III. THEORY FOR THE TIME CORRELATION FUNCTION

As discussed earlier, in this paper we develop a short-time expansion for the classical TCF in Eq. (15). This expansion involves only even powers of time, and can be written as[65]

$$C(t)=\sum_{n=0}^{\infty}\frac{(-1)^n}{(2n)!}C_{2n}t^{2n}. \tag{19}$$

C_0 is given by

$$C_0=C(0)=\langle F^2\rangle-\langle F\rangle^2, \tag{20}$$

and the other coefficients, by

$$C_{2n}=\left\langle\left(\frac{d^nF}{dt^n}\right)^2\right\rangle. \tag{21}$$

The general approach to calculating these coefficients has been described by several authors.[63,73,74] Let us begin by considering C_0. Using Eq. (10) and the indistinguishability of the solvent particles, the above expression can be separated into terms involving one and two solvent atoms

$$C_0=N\langle f(r_{10})^2\rangle+N(N-1)\langle f(r_{10})f(r_{20})\rangle - (N\langle f(r_{10})\rangle)^2. \tag{22}$$

Making the Kirkwood superposition approximation for the three-body solute–solvent–solvent distribution function, and taking the thermodynamic limit, gives

$$C_0=\rho\int d\vec{r}f(r)^2g(r) + \rho^2\int d\vec{r}_1d\vec{r}_2f(r_1)f(r_2)g(r_1)g(r_2)h_s(r_{12}), \tag{23}$$

where ρ is the solvent number density, $g(r)$ and $g_s(r)$ are, respectively, the solute–solvent and solvent–solvent radial distribution functions, and $h_s(r)=g_s(r)-1$.

Next consider $C_2=\langle\dot{F}^2\rangle$, where $F\equiv dF/dt$. From Eq. (10) $\dot{F}=\Sigma_i\dot{f}(r_{i0})$. $\dot{f}(r)$ can be evaluated with the chain rule

$$\dot{f}(r)=f'(r)\dot{r}=f'(r)(\hat{r}\cdot\vec{v}), \tag{24}$$

where $\hat{r}=\vec{r}/r$ and $\vec{v}=\dot{\vec{r}}$. Thus we find that

$$C_2=N\langle f'(r_{10})^2(\hat{r}_{10}\cdot\vec{v}_{10})^2\rangle+N(N-1)\langle f'(r_{10}) \times(\hat{r}_{10}\cdot\vec{v}_{10})f'(r_{20})(\hat{r}_{20}\cdot\vec{v}_{20})\rangle, \tag{25}$$

where $\vec{r}_{ij}=\vec{r}_i-\vec{r}_j$. This formula is similar to that for C_0, the important difference being that it involves averages over velocities. These averages can be performed independently of the spatial averages, to obtain

$$C_2=\frac{\rho kT}{\mu}\int d\vec{r}f'(r)^2g(r)+\frac{\rho^2kT}{m_0}\int d\vec{r}_1d\vec{r}_2f'(r_1) \times f'(r_2)(\hat{r}_1\cdot\hat{r}_2)g(r_1)g(r_2)g_s(r_{12}). \tag{26}$$

μ is the solute–solvent reduced mass: $\mu=m_0m_s/(m_0+m_s)$.

The calculation of C_4 is substantially more difficult because it involves the accelerations of the particles. The final result and a sketch of the derivation are given in Appendix A.

Thus, we now have microscopic expressions for the terms of order t^2 and t^4 in the series expansion of the TCF. Defining

$$A=\frac{C_2}{2C_0},\qquad B=\frac{C_4}{24C_0}, \tag{27}$$

we can write the normalized TCF as

$$\overline{C(t)}=\frac{C(t)}{C(0)}=1-At^2+Bt^4+\cdots. \tag{28}$$

One possible way to proceed further is to introduce an analytical ansatz for $C(t)$ that will incorporate the information about the short-time behavior contained in A and B. Following Douglass[67] we approximate $\overline{C(t)}$ by

$$\overline{C(t)}=\frac{\cos(bt)}{\cosh(at)}. \tag{29}$$

The parameters a and b are determined by the requirement that this ansatz has the same short-time expansion (through order t^4) as Eq. (28). Under this condition, a and b are given in terms of A and the dimensionless ratio $\lambda=B/A^2$ by the following formulas

$$a^2=(3\lambda-1/2)A,\qquad b^2=(5/2-3\lambda)A. \tag{30}$$

Note that for $\lambda>5/6$ the parameter b becomes purely imaginary, and $C(t)$, while decaying to zero at long times (since $a>|b|$) stays positive. Note also that for $\lambda<1/6$, a becomes purely imaginary, and $C(t)$ displays an oscillatory behavior and does not decay to zero. Therefore, λ must be greater than 1/6 for this approach to be meaningful.

The formula for the VER rate, Eq. (18), can be written as

$$\frac{1}{T_1}=\frac{2C_0\tanh(\beta\hbar\omega/2)}{\hbar\omega m}\hat{C}(\omega), \tag{31}$$

where

$$\hat{C}(\omega)\equiv\int_0^{\infty}dt\cos(\omega t)\overline{C(t)}. \tag{32}$$

The Fourier transform of $\overline{C(t)}$ given in Eq. (29) can be performed analytically to yield[75]

$$\hat{C}(\omega)=\left(\frac{\pi}{a}\right)\frac{\cosh(\pi\omega/2a)\cosh(\pi b/2a)}{\cosh(\pi\omega/a)+\cosh(\pi b/a)}. \tag{33}$$

This expression makes it possible to discuss the dependence of the rate on various factors. We start by analyzing the dependence of T_1^{-1} on the vibrational frequency of the diatomic, ω. For ω somewhat larger than a (and b, if b is real), from the above we see that

$$\frac{1}{T_1} \simeq \frac{2\pi C_0 \tanh(\beta\hbar\omega/2)}{a\hbar\omega m} \cosh(\pi b/2a)\exp(-\pi\omega/2a). \tag{34}$$

The frequency dependence of T_1^{-1} is dominated by the exponential, and thus, the theoretical ansatz gives a nearly exponential ''energy gap law.'' If the classical limit ($\hbar\omega$ small compared to kT) can be satisfied at the same time, then

$$\frac{1}{T_1} \simeq \frac{\pi C_0}{amkT} \cosh(\pi b/2a)\exp(-\pi\omega/2a), \tag{35}$$

which decreases strictly exponentially with ω.

For a particular diatomic, the value of the vibrational frequency is fixed. Among other factors that affect the relaxation rate are the thermodynamic parameters of the solvent—namely, its density and temperature. The microscopic parameters C_0, a, and b depend on these explicitly and also through the radial distribution functions. For high frequencies the rate is most sensitive to C_0 and to a. The rate is proportional to C_0, which is equal to the variance of the fluctuating force, and which is expected to increase with increasing temperature or with increasing density. a is essentially the decay rate of the TCF, which also is expected to increase with increasing temperature or density. For high frequencies our expression for the rate shows that the rate increases with increasing a. This is because a TCF with a faster decay rate has larger high frequency Fourier components. Thus the variations of both C_0 and a with density or temperature indicate that the rate should increase with increasing density or temperature.

IV. RESULTS FOR THE TCF: COMPARISON BETWEEN THEORY AND MOLECULAR DYNAMICS SIMULATION

The theory for the force–force TCF described above involves the ansatz in Eq. (29). While this ansatz is guaranteed to give the correct short- and intermediate-time behavior, its accuracy at long times needs to be assessed. For this reason we compare our theoretical result for the TCF with exact results from a molecular dynamics simulation. To this end, and also to enable a comparison of our theory with experiment, we must choose specific forms for the solvent–solvent and solute–solvent potentials.

We assume that the solvent atoms interact with each other with the familiar Lennard-Jones form

$$\phi_s(r) = 4\epsilon_s\left[\left(\frac{\sigma_s}{r}\right)^{12} - \left(\frac{\sigma_s}{r}\right)^{6}\right], \tag{36}$$

where ϵ_s is the well depth and σ_s is the effective diameter of the solvent particle.

The solute can also be characterized by an effective diameter. In our breathing sphere model of the solute we assume that this diameter is $\sigma_0+\alpha q$, where σ_0 is (obviously) the value of the solute's diameter when $q=0$, and α is a (dimensionless) parameter. If the solute and its vibration were truly spherical, then it would be appropriate to simply set $\alpha=1$. However, a diatomic molecule expands and contracts in only one dimension. To model this situation by an effective breathing sphere, it is clear that α should be less than (but on the order of) unity. In comparing our theory to experiment, we will treat α as an adjustable parameter. We next assume that the solute interacts with solvent atoms with another Lennard-Jones potential. For a pair of unlike atoms or molecules it is customary to use standard combining rules to determine Lennard-Jones parameters. Thus, the well depth for the unlike pair is the geometric average of the well depths for each species, and the effective diameter is the arithmetic average of the two diameters.[76] In this spirit, for the q-dependent solute–solvent interaction potential we write

$$\phi(r,q) = 4\epsilon\left[\left(\frac{\sigma_s+\sigma_0+\alpha q}{2r}\right)^{12} - \left(\frac{\sigma_s+\sigma_0+\alpha q}{2r}\right)^{6}\right], \tag{37}$$

where $\epsilon=\sqrt{\epsilon_0\epsilon_s}$, and ϵ_0 is the solute–solute well depth. From this we obtain

$$\phi(r) = \phi(r,0) = 4\epsilon\left[\left(\frac{\sigma}{r}\right)^{12} - \left(\frac{\sigma}{r}\right)^{6}\right], \tag{38}$$

and

$$f(r) = -\left.\frac{\partial\phi(r,q)}{\partial q}\right|_{q=0} = -\frac{12\epsilon\alpha}{\sigma}\left[2\left(\frac{\sigma}{r}\right)^{12} - \left(\frac{\sigma}{r}\right)^{6}\right], \tag{39}$$

where $\sigma=(\sigma_0+\sigma_s)/2$.

In addition to these potentials, the only other quantities needed for the theoretical calculation of the TCF are the solvent–solvent and solute–solvent (at infinite solute dilution) radial distribution functions. We have recently shown,[70] for several Lennard-Jones mixtures at several thermodynamic states of the solvent, that the HMSA integral equation theory proposed by Zerah and Hansen[69] gives excellent results for these quantities. Accordingly, in this study we employ this method.

For the above model, the special case $\sigma_0=\sigma_s=\sigma$, $\epsilon_0=\epsilon_s=\epsilon$ and $m_0=m_s=\tilde{m}$ corresponds to a neat fluid. In this case, of course, $g_s(r)=g(r)$. In comparing theory with molecular dynamics simulation, we employ the above simplification since it allows us to treat each particle in the liquid as a solute and thereby improves the simulation statistics considerably. For the purposes of this comparison we set $\alpha=1$. To present our results, we define the dimensionless spatial, time and frequency variables as follows: $r^*=r/\sigma$, $t^*=t(\epsilon/\tilde{m}\sigma^2)^{1/2}$ and $\omega^*=\omega(\tilde{m}\sigma^2/\epsilon)^{1/2}$. Note, for example, that for Ar, $\omega^*=1$ corresponds to $\omega/2\pi c=2.46\ \mathrm{cm}^{-1}$. The dimensionless density and temperature are defined by $\rho^*=\rho\sigma^3$ and $T^*=kT/\epsilon$.

The phase diagram for the Lennard-Jones fluid is known from simulation data;[77] it is reproduced in Fig. 1. We perform molecular dynamics simulations for three particular sets of thermodynamic parameters, as shown by squares in Fig. 1 and listed in Table I. The velocity-Verlet algorithm[78] is used to integrate the equations of motion for a liquid of 864 particles in a cubic box employing periodic boundary conditions and the minimum image convention. The dimensionless box length is equal to $(864/\rho^*)^{1/3}$, and the pair po-

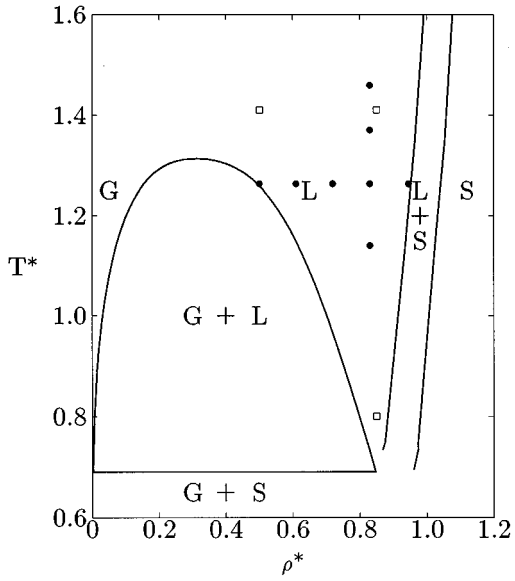

FIG. 1. The Lennard-Jones phase diagram. Squares indicate the points at which we performed molecular dynamics simulations. Solid circles indicate the points at which experiments in Xe (taking σ=3.930 Å, ϵ=221.7 K) were performed (Ref. 13).

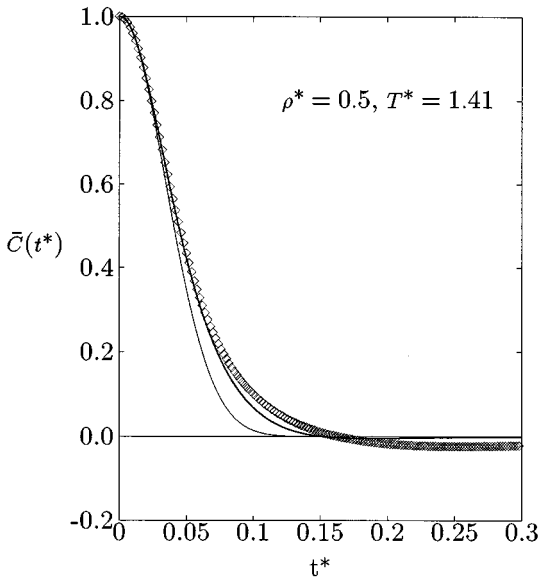

FIG. 2. Normalized force–force correlation function, $\overline{C}(t^*)$, vs t^*. The diamonds are the simulation results, the thick line is from the theoretical ansatz in Eq. (29), and the thin line is from the Gaussian ansatz, as described in the text. The solvent density and temperature are ρ^*=0.5 and T^*=1.41.

tential is truncated at half of this value. The system is propagated with a time step of δt^*=0.002. For each thermodynamic state we calculate the force–force TCF from the simulation. The initial values, $C_0^* = C_0\sigma^2/\epsilon^2$, are given in Table I, and the normalized correlation functions are shown in Figs. 2–4.

For each set of thermodynamic parameters we also calculate the theoretical TCF. The radial distribution function is calculated as described above. With this, C_0, C_2, and C_4 are obtained from Eqs. (23), (26), and (A7) by numerical integration. These parameters determine the coefficients A and B, which in turn lead to a and b. The values of C_0^*, $a^* = a(\tilde{m}\sigma^2/\epsilon)^{1/2}$ and $b^* = b(\tilde{m}\sigma^2/\epsilon)^{1/2}$ are shown in Table I. It is seen that the agreement between the theoretical and simulation values for C_0^* is excellent. In view of the superposition approximation inherent in the second term of Eq. (23) this level of agreement is somewhat surprizing. In fact, for these calculations the first term in Eq. (23) dominates, and since $g(r)$ is given very accurately by the HMSA theory, this good agreement is to be expected. From the calculated values of a and b we obtain the theoretical normalized TCF from Eq. (29). For the three thermodynamic points, these are also shown in Figs. 2–4. As expected, the theoretical TCF has the correct short- and intermediate-time behavior. At longer times it decays to zero faster than the simulation result. For comparison, we also show results for the Gaussian ansatz, $C(t)=\exp(-At^2)$, which involves only the first two coefficients in the short-time expansion of the TCF. In all cases it is seen to decay substantially too fast.

The VER rate is proportional to $\hat{C}(\omega)$, the cosine transform of $C(t)$, which is defined by Eq. (32). For the simulated TCFs for the three thermodynamic points, these transforms are obtained numerically, and the results are shown in Figs. 5–7. The theoretical results, given by Eq. (33), are also shown in these figures. The agreement between theory and simulation is quite good in all cases, and excellent for the

TABLE I. Microscopic parameters for the force–force TCF.

ρ^*	T^*	C_0^* from sim.	C_0^* from theory	a^*	b^*
0.50	1.41	144±2	144	27.12	10.33
0.85	1.41	382±2	384	30.15	1.40i
0.85	0.80	173±1	178	23.96	5.72i

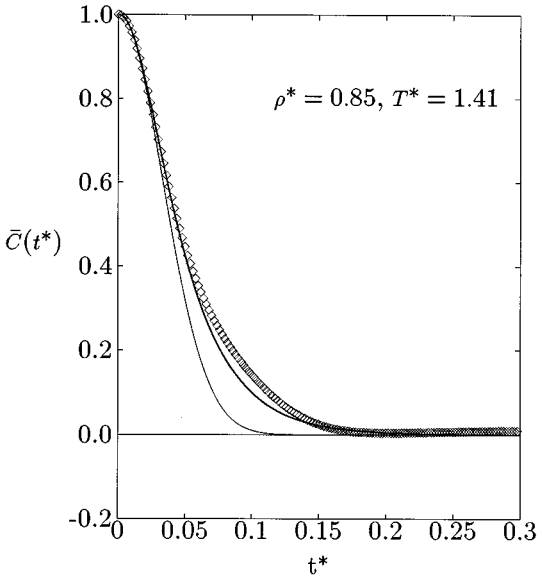

FIG. 3. Same as Fig. 2 but for ρ^*=0.85 and T^*=1.41.

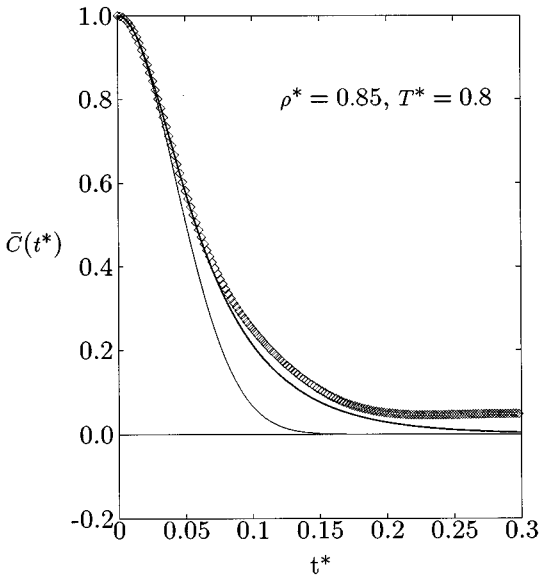

FIG. 4. Same as for Fig. 2 but for $\rho^*=0.85$ and $T^*=0.8$.

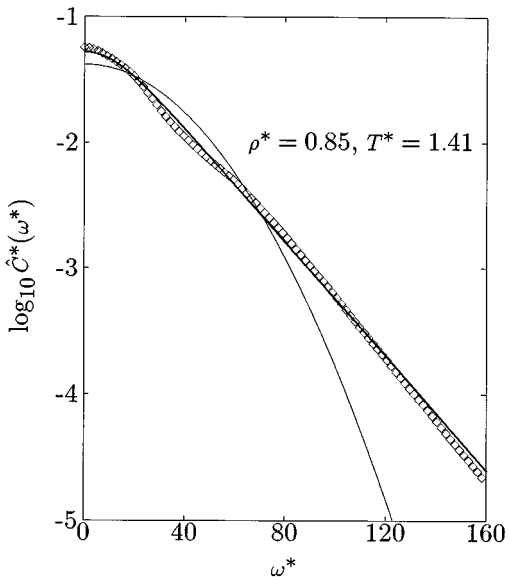

FIG. 6. Same as Fig. 5 but for $\rho^*=0.85$ and $T^*=1.41$.

point at high temperature and low density. One can see that for $\omega > a$, $\hat{C}(\omega)$ decreases exponentially with ω, as discussed earlier. For comparison we also show $\hat{C}(\omega)$ for the Gaussian ansatz: $\hat{C}(\omega)=(\pi/4A)^{1/2}\exp(-\omega^2/4A)$. As discussed in the Introduction, for all but the lowest frequencies this ansatz is inaccurate, underestimating $\hat{C}(\omega)$, and hence the VER rate, quite dramatically.

The conclusion of this comparison between theory and simulation is that for a wide range of temperatures and densities, the Fourier transform of the theoretical TCF, which is the relevant quantity for the VER rate, is remarkably accurate. Buoyed by this success, in the next section we will analyze some experimental results with the theory.

V. THE VER RATE: COMPARISON BETWEEN THEORY AND EXPERIMENT

We first consider VER of molecular iodine in fluid xenon. In terms of experimental data available, it is one of the most thoroughly studied systems.[10–13] As far as theoretical analysis is concerned, it fits into the framework of our microscopic model (diatomic solute in monatomic solvent). The I_2 molecule is sufficiently heavy that neglecting the effect of its rotation should be a reasonable approximation. Classical treatment of the solvent in the temperature range

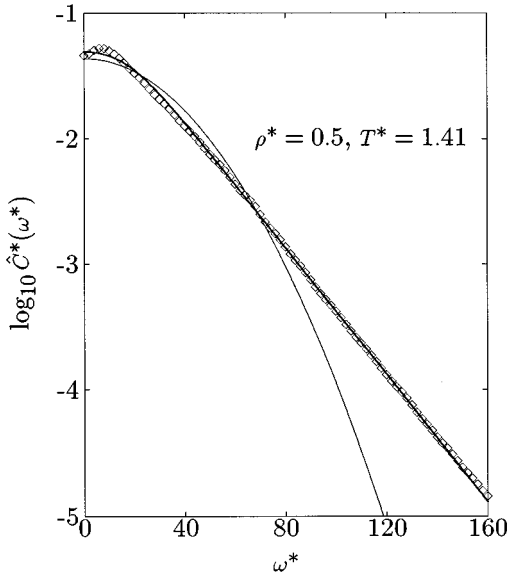

FIG. 5. $\hat{C}^*(\omega^*)$ vs ω^*. The diamonds are the simulation results, the thick line is from the theoretical ansatz in Eq. (33), and the thin line is from the Gaussian ansatz, as described in the text. The solvent density and temperature are $\rho^*=0.5$ and $T^*=1.41$.

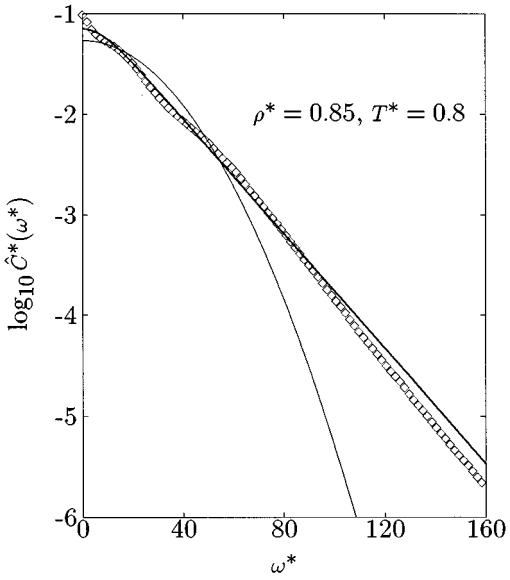

FIG. 7. Same as for Fig. 5 but for $\rho^*=0.85$ and $T^*=0.8$.

TABLE II. Measured relaxation rates for I_2 in Xe; the error bars for the experimental values are two standard deviations.

ρ (g/cm^3)	T (K)	$1/T_1$ (10^9 s^{-1})
1.8	280	0.40±0.06
2.2	280	0.71±0.14
2.6	280	0.77±0.12
3.0	280	1.20±0.22
3.4	280	1.79±0.38
3.0	253	0.85±0.17
3.0	303	1.82±0.40
3.0	323	1.89±0.46

considered below also seems justified. Finally, the model based on Lennard-Jones potentials can be expected to describe xenon reasonably well.

We analyze the experimental data of Paige and Harris,[13] who studied the VER rate of I_2 in liquid Xe at 280 K for a variety of solvent densities from 1.8 to 3.4 g/cm^3, and at a density of 3.0 g/cm^3 for several temperatures from 253 to 323 K. Their results for $1/T_1$ are given in Table II. To obtain these numbers from the published data, we first focused on the relaxation curve for $\rho=1.8$ g/cm^3 and $T=280$ K. We define T_1 to be the time when the average energy falls to $1/e$ of its initial value (even if the decay is not strictly exponential); for this particular thermodynamic point we find that $1/T_1=0.4\times10^9$ s^{-1}. The error bar for this value, and the values for $1/T_1$ and their associated error bars for all of the other thermodynamic states of the solvent are obtained from the published ''time-scaling'' factors.[13]

To implement our theory we use the Lennard-Jones solute–solvent and solvent–solvent interaction potentials described in Sec. IV. We take the following Lennard-Jones parameters for the solute[79] and the solvent: $\epsilon_{I_2}/k=\epsilon_0/k=550$ K, $\sigma_{I_2}=\sigma_0=4.982$ Å; $\epsilon_{Xe}/k=\epsilon_s/k=221.7$ K, $\sigma_{Xe}=\sigma_s=3.930$ Å. With these parameters for Xe, which were chosen to match the experimental liquid–gas and liquid–solid coexistence densities at 280 K,[13] the range of solvent densities and temperatures studied experimentally corresponds to $\rho^*=0.50$ to 0.95 and $T^*=1.14$ to 1.46. (All dimensionless quantities in this section are defined in terms of the solvent Lennard-Jones parameters). The particular values of densities and temperatures for the experiments of Paige and Harris are shown by solid circles on the phase diagram of Fig. 1. The solute and solvent masses are, respectively: $m_{I_2}=m_0=4.22\times10^{-22}$ g, and $m_{Xe}=m_s=2.18\times10^{-22}$ g. The vibrational frequency of molecular iodine is $\omega/2\pi c=214.6$ cm^{-1},[80] and the reduced mass, m, for the vibrational mode is equal to $m_0/4$.

To compare with experiment we perform calculations at fixed density ($\rho=3.0$ g/cm^3; $\rho^*=0.83$) as a function of temperature, and at fixed temperature ($T=280$ K; $T^*=1.26$) as a function of density. For each thermodynamic state we calculate the solute–solvent and solvent–solvent radial distribution functions from theory,[70] and using these, obtain the parameters C_0, a, and b following the procedure described in Sec. IV. With these, we calculate the relaxation rates from

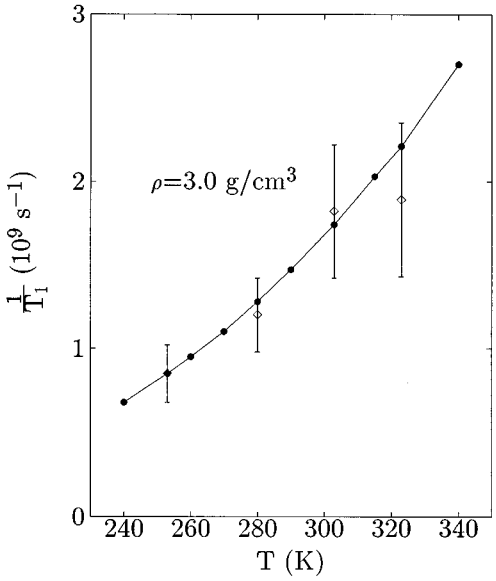

FIG. 8. $1/T_1$ vs T at $\rho=3.0$ g/cm^3. The diamonds are the experimental points, and the solid circles (with connecting lines) are from theory.

Eqs. (31) and (33). α is adjusted to give the best overall agreement between theory and experiment; this procedure gives $\alpha=0.7$, which (see the discussion in Sec. IV) is a reasonable value. In Fig. 8 we compare our theoretical results for $1/T_1$ with the constant density experimental results. The corresponding constant temperature comparison is shown in Fig. 9. The agreement between theory and experiment at constant density is excellent. The agreement at constant temperature is quite satisfactory, although the theoretical density dependence is steeper than that observed experimentally.

The experimental rates can also be compared to theoretical results from a classical molecular dynamics simulation,[41]

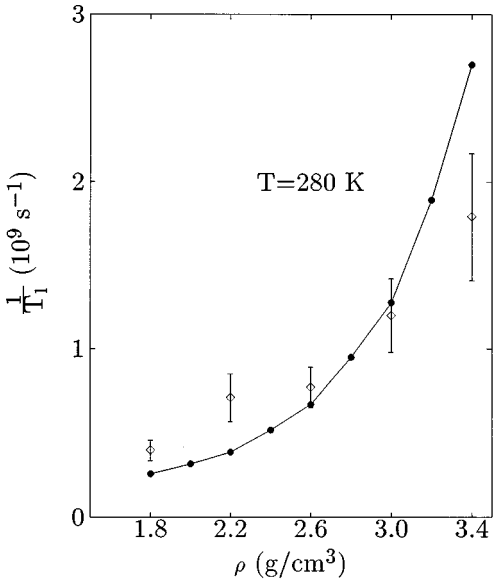

FIG. 9. $1/T_1$ vs ρ at $T=280$ K. The diamonds are the experimental points, and the solid circles (with connecting lines) are from theory.

which give VER rates about an order of magnitude too fast. This discrepancy must be due either to inaccuracies in the potential function or to the classical approximation of the oscillator's motion. On the other hand, the Gaussian theory of Adelman *et al.*[62] gives relaxation rates that are about an order of magnitude too slow. This is consistent with our simulation results, which show that the Gaussian approximation underestimates VER rates.

In addition to the system considered above, we have also studied VER of molecular oxygen in liquid argon. The relaxation rate for the first excited vibrational state of O_2 has been measured by Faltermeier *et al.*[2] in liquid O_2–Ar mixtures for the range of O_2 mole fractions from 0.25 to 1.0. By extrapolating the data to the infinitely dilute system, they obtained the relaxation time $T_1=0.08$ s at $T=77$ K. In fact, argon is solid at this temperature; its melting and boiling points at one atmosphere are, respectively, 83.8 and 87.3 K.[81] For these two points, we calculate T_1 from the first excited vibrational state of O_2 assuming that it is present at infinite dilution in liquid argon. In performing the calculation, we follow the procedure outlined above for I_2–Xe system. We take the following values for the solute and the solvent Lennard-Jones parameters:[79] $\epsilon_{O_2}/k=\epsilon_0/k=117.5$ K, $\sigma_{O_2}=\sigma_0=3.580$ Å; $\epsilon_{Ar}/k=\epsilon_s/k=119.8$ K, $\sigma_{Ar}=\sigma_s=3.405$ Å. With these parameters for Ar, the reduced Lennard-Jones density and temperature at the melting point are $\rho^*=0.843$, $T^*=0.699$, and at the boiling point, $\rho^*=0.831$, $T^*=0.729$. The solute and solvent masses are, respectively: $m_{O_2}=m_0=5.32\times10^{-23}$ g, $m_{Ar}=m_s=6.63\times10^{-23}$ g. The vibrational frequency of molecular oxygen (for the $0\rightarrow1$ transition) is $\omega/2\pi c=1556$ cm^{-1}.[80] Taking $\alpha=0.7$ (as above), at the melting point we obtain $T_1=1.7\times10^5$ s, and at the boiling point, $T_1=1.3\times10^5$ s. Both values are much larger than the (extrapolated) experimental value of $T_1=0.08$ s. In our defense we might mention that a molecular calculation of relaxation times on the order of seconds, when the fundamental molecular time scale is subpicosecond, is extremely challenging. Possible reasons for the large discrepancy between the calculated and measured relaxation times are numerous. First, modeling the diatomic as a ''breathing sphere'' could have more serious consequences for this case than for the I_2–Xe system: the oxygen molecule mass is comparable to that of argon, and the rotation of the diatomic could contribute significantly to the relaxation rate. Furthermore, of course, the actual shape of the diatomic is oblong rather than spherical; taking this into account would shift the first peak of the solute–solvent radial distribution function to shorter distances and would surely affect the microscopic parameters of our model. At the high frequencies of O_2 the theoretical results are extremely sensitive to these parameters, especially a. Secondly, to calculate the relaxation time we use a phenomenological model for the time correlation function that gives an exponential ''energy gap'' dependence. The validity of this result can only be tested in the frequency range where the TCF from a molecular dynamics simulation can be Fourier transformed numerically. The vibrational frequency of molecular oxygen is well outside this range, and therefore, the applicability of our phenomenological model could be questionable. Thirdly, Faltermeier *et al.*[3] argue that O_2–O_2 interactions play an important role in the relaxation process even for the lowest O_2 mole fraction studied. In particular, O_2 vibrational energy can be transferred to rotations of surrounding oxygen molecules; therefore, a straightforward extrapolation of the experimental data to the infinite dilution limit could be problematic, and the actual experimental T_1 at infinite dilution might be substantially longer than 0.08 s. Finally, at these low temperatures (compared to ϵ_s/k), the assumption of a classical solvent may also be questionable. One way to clarify some of these issues would be to incorporate into the model the true diatomic nature of the solute. In principle, the model could also be extended to treat solutes at finite mole fraction. We hope to tackle these problems in the future.

VI. CONCLUDING REMARKS

In this paper, we have developed a microscopic treatment of vibrational energy relaxation in liquids based on the force–force time-correlation function approach. Our theory involves a short-time expansion of the correlation function. In particular, for our breathing sphere model we calculate the first three nonvanishing terms in this expansion. This information is incorporated into a phenomenological ansatz for the full time dependence of the correlation function. We obtain a nearly exponential dependence of the vibrational relaxation rate on the vibrational frequency.

With our microscopic model we analyzed experimental data on the vibrational relaxation of molecular iodine in xenon. The experimentally observed relaxation rate and its density and temperature dependences over much of the fluid region of the phase diagram are reproduced quite well by our theory.

The application of our model to vibrational relaxation of molecular oxygen in liquid argon has revealed a large discrepancy between the measured and calculated relaxation times. This fact points to the possible limitations of the breathing sphere model, and indicates that refinements of the theory are probably necessary.

NOTES ADDED IN PROOF

Equation (18) for the VER rate comes from making a semiclassical approximation to the exact quantum mechanical result. In the classical limit ($kT \gg \hbar\omega$) this will certainly be correct. However, one often (as in this paper) wants to use this formula when this limit does not obtain. In Ref. 72 Bader and Berne showed that if the solvent can be represented by an effective harmonic bath, then in order to recover the exact solution to this harmonic model, Eq. (18) must be multiplied by the factor $(\hbar\omega/2kT)\coth(\hbar\omega/2kT)$. If the solvent can be represented by an effective harmonic bath then the fluctuating force describes a Gaussian process. One indication of this is that the distribution of forces is Gauss-

ian. We have calculated the distribution of forces from our simulation for the neat fluid at $\rho^* = 0.5$ and $T^* = 1.41$, and find that the distribution is very asymmetric. For our model of I_2 in Xe at $\rho = 3.0$ g/cm^3 and $T = 280$ K the distribution of forces is less asymmetric, but still not very Gaussian. In any case, for this system the correction factor is only 1.09. For our model for O_2 in Ar the distribution of forces is closer to Gaussian, and the coarection factor is about 14. Multiplying our results by this factor leads to T_1 on the order of 10^4 s, which is closer to the experimental relaxation times, but still way too long.

The inaccuracy of the time-dependent Gaussian ansatz for calculating VER rates was pointed out previously by M. Bruehl and J. T. Hynes, Chem. Phys. **175**, 205 (1993).

ACKNOWLEDGMENTS

J.L.S. is grateful for support from the National Science Foundation (Grants Nos. CHE-9522057 and CHE-9526815) and from the Humboldt Foundation. J.L.S also acknowledges the gracious hospitality of Sepp Friedrich and Dietrich Haarer at the University of Bayreuth, where the final version of this paper was completed. J.L.S. is indebted to Professor Bruce Berne for an especially illuminating discussion regarding the first note added in proof. J.L.S. thanks Professor Casey Hynes for the refrence in the second note added in proof, and also for several helpful suggestions regarding the text.

APPENDIX A

It proves most convenient to derive the result for C_4 from the expression

$$C_4 = -\left\langle \left(\frac{dF}{dt}\right)\left(\frac{d^3F}{dt^3}\right)\right\rangle, \tag{A1}$$

which is completely equivalent to that given in Sec. III.[82] $d^3F/dt^3 = \Sigma_i (d^3 f(r_{i0})/dt^3)$, and so, as before, we can write

$$C_4 = -N\left\langle \left(\frac{df(r_{10})}{dt}\right)\left(\frac{d^3 f(r_{10})}{dt^3}\right)\right\rangle - N(N-1) \times \left\langle \left(\frac{df(r_{20})}{dt}\right)\left(\frac{d^3 f(r_{10})}{dt^3}\right)\right\rangle. \tag{A2}$$

With the help of the chain rule we find that

$$\frac{d^3 f(r)}{dt^3} = f'''(r)(\hat{r}\cdot\vec{v})^3 + 3f''(r)(\hat{r}\cdot\vec{v})\left(\frac{v^2-(\hat{r}\cdot\vec{v})^2}{r} + (\hat{r}\cdot\vec{a})\right) + 3f'(r)\left(\frac{(\vec{v}\cdot\vec{a})-(\hat{r}\cdot\vec{a})(\hat{r}\cdot\vec{v})}{r} + \frac{(\hat{r}\cdot\vec{v})^3 - v^2(\hat{r}\cdot\vec{v})}{r^2}\right) + f'(r)(\hat{r}\cdot\dot{\vec{a}}), \tag{A3}$$

where $\vec{a} = \dot{\vec{v}}$.

The acceleration $\vec{a}_{10}$ is given by

$$\vec{a}_{10} = \frac{\vec{\nabla}_0 U_0}{m_0} - \frac{\vec{\nabla}_1 U_0}{m_s}. \tag{A4}$$

From this result one can derive, with a suitable integration by parts, the following identity:

$$\langle \vec{G}(\vec{r}_0 \cdots \vec{r}_N)\cdot\vec{a}_{10}\rangle = kT\left\langle \left(\frac{\vec{\nabla}_0}{m_0} - \frac{\vec{\nabla}_1}{m_s}\right)\cdot\vec{G}(\vec{r}_0\cdots\vec{r}_N)\right\rangle, \tag{A5}$$

which is helpful in evaluating several of the terms above.

On the other hand, terms involving $\dot{\vec{a}}_{10}$ need to be considered explicitly. Using the chain rule one finds that

$$\dot{\vec{a}}_{10} = -\frac{1}{\mu}\left[\left(\phi''(r_{10}) - \frac{\phi'(r_{10})}{r_{10}}\right)(\hat{r}_{10}\cdot\vec{v}_{10})\hat{r}_{10} + \frac{\phi'(r_{10})}{r_{10}}\vec{v}_{10}\right] - \frac{1}{m_s}\sum_{j=2}^{N}\left[\left(\phi_s''(r_{1j}) - \frac{\phi_s'(r_{1j})}{r_{1j}}\right)(\hat{r}_{1j}\cdot\vec{v}_{1j})\hat{r}_{1j} + \frac{\phi'(r_{1j})}{r_{1j}}\vec{v}_{1j}\right] - \frac{1}{m_0}\sum_{j=2}^{N}\left[\left(\phi''(r_{j0}) - \frac{\phi'(r_{j0})}{r_{j0}}\right)(\hat{r}_{j0}\cdot\vec{v}_{j0})\hat{r}_{j0} + \frac{\phi'(r_{j0})}{r_{j0}}\vec{v}_{j0}\right]. \tag{A6}$$

Velocity averages of products of four velocities can be simplified by using the Gaussian nature of the velocity distributions. After some algebra the final result for C_4 is

$$C_4=\rho\left(\frac{kT}{\mu}\right)^2\int d\vec{r}\left\{3f''(r)^2+6\frac{f'(r)^2}{r^2}+\frac{f'(r)^2\phi''(r)}{kT}\right\}g(r)+\rho^2kT\int d\vec{r}_1d\vec{r}_2f'(r_1)^2\left\{\frac{1}{m_0^2}\left[\left(\phi''(r_2)-\frac{\phi'(r_2)}{r_2}\right)(\hat{r}_1\cdot\hat{r}_2)^2+\frac{\phi'(r_2)}{r_2}\right]+\frac{1}{m_s^2}\left[\left(\phi_s''(r_{12})-\frac{\phi_s'(r_{12})}{r_{12}}\right)(\hat{r}_1\cdot\hat{r}_{12})^2+\frac{\phi_s'(r_{12})}{r_{12}}\right]\right\}g(r_1)g(r_2)g_s(r_{12})$$
$$+\rho^2\left(\frac{kT}{m_0}\right)^2\int d\vec{r}_1d\vec{r}_2\left\{3f''(r_1)f''(r_2)(\hat{r}_1\cdot\hat{r}_2)^2+6\frac{f'(r_1)f''(r_2)}{r_1}(1-(\hat{r}_1\cdot\hat{r}_2)^2)+3\frac{f'(r_1)f'(r_2)}{r_1r_2}(1+(\hat{r}_1\cdot\hat{r}_2)^2)\right.$$
$$\left.+2\frac{m_0}{\mu kT}f'(r_1)f'(r_2)\phi''(r_1)(\hat{r}_1\cdot\hat{r}_2)\right\}g(r_1)g(r_2)g_s(r_{12})-\rho^2\frac{kT}{m_s^2}\int d\vec{r}_1d\vec{r}_2f'(r_1)f'(r_2)\left\{\left(\phi_s''(r_{12})-\frac{\phi_s'(r_{12})}{r_{12}}\right)\right.$$
$$\left.\times(\hat{r}_1\cdot\hat{r}_{12})(\hat{r}_2\cdot\hat{r}_{12})+\frac{\phi_s'(r_{12})}{r_{12}}(\hat{r}_1\cdot\hat{r}_2)\right\}g(r_1)g(r_2)g_s(r_{12})+\rho^3\frac{kT}{m_0^2}\int d\vec{r}_1d\vec{r}_2d\vec{r}_3f'(r_1)f'(r_2)\left\{\left(\phi''(r_3)-\frac{\phi'(r_3)}{r_3}\right)\right.$$
$$\left.\times(\hat{r}_1\cdot\hat{r}_3)(\hat{r}_2\cdot\hat{r}_3)+\frac{\phi'(r_3)}{r_3}(\hat{r}_1\cdot\hat{r}_2)\right\}g(r_1)g(r_2)g(r_3)g_s(r_{12})g_s(r_{13})g_s(r_{23}). \quad \text{(A7)}$$

In the last term (that of order ρ^3) we have used the Kirkwood hypersuperposition approximation to write the four-body distribution function as a product of six pair distribution functions.

Numerical results show that the contribution from the terms of order ρ^2 does not exceed 10% of the term of order ρ. Assuming that the ρ^3 term is similarly small compared to the ρ^2 terms, in our numerical calculations of C_4 we simply neglect this (the ρ^3) term.

[1] A. Laubereau and W. Kaiser, Rev. Mod. Phys. **50**, 607 (1978).
[2] B. Faltermeier, R. Protz, M. Maier, and E. Werner, Chem. Phys. Lett. **74**, 425 (1980).
[3] B. Faltermeier, R. Protz, and M. Maier, Chem. Phys. **62**, 377 (1981).
[4] M. Chateau *et al.*, J. Chem. Phys. **71**, 4799 (1979).
[5] C. Delalande and G. M. Gale, J. Chem. Phys. **73**, 1918 (1980).
[6] P. Roussignol, C. Delalande, and G. M. Gale, Chem. Phys. **70**, 319 (1982).
[7] E. J. Heilweil, M. P. Casassa, R. R. Cavanagh, and J. C. Stephenson, Chem. Phys. Lett. **117**, 185 (1985).
[8] E. J. Heilweil, M. P. Casassa, R. R. Cavanagh, and J. C. Stephenson, J. Chem. Phys. **85**, 5004 (1986).
[9] E. J. Heilweil, F. E. Doany, R. Moore, and R. M. Hochstrasser, J. Chem. Phys. **76**, 5632 (1982).
[10] A. L. Harris, J. K. Brown, and C. B. Harris, Annu. Rev. Phys. Chem. **39**, 341 (1988).
[11] M. E. Paige, D. J. Russell, and C. B. Harris, J. Chem. Phys. **85**, 3699 (1986).
[12] M. E. Paige and C. B. Harris, J. Chem. Phys. **93**, 3712 (1990).
[13] M. E. Paige and C. B. Harris, Chem. Phys. **149**, 37 (1990).
[14] A. Moustakas and E. Weitz, J. Chem. Phys. **98**, 6947 (1993).
[15] D. Zimdars *et al.*, Phys. Rev. Lett. **70**, 2718 (1993).
[16] A. Tokmakoff, B. Sauter, and M. D. Fayer, J. Chem. Phys. **100**, 9035 (1994).
[17] N. Pugliano, A. Z. Szarka, S. Gnanakaran, and R. M. Hochstrasser, J. Chem. Phys. **103**, 6498 (1995).
[18] W. F. Calaway and G. E. Ewing, J. Chem. Phys. **63**, 2842 (1975).
[19] S. R. J. Brueck and R. M. Osgood, Chem. Phys. Lett. **39**, 568 (1976).
[20] D. A. V. Kliner, J. C. Alfano, and P. F. Barbara, J. Chem. Phys. **98**, 5375 (1993).
[21] J. C. Owrutsky *et al.*, Chem. Phys. Lett. **184**, 368 (1991).
[22] D. Oxtoby, Adv. Chem. Phys. **47** (part 2), 487 (1981).
[23] D. W. Oxtoby, Annu. Rev. Phys. Chem. **32**, 77 (1981).
[24] D. W. Oxtoby, J. Phys. Chem. **87**, 3028 (1983).
[25] J. Chesnoy and G. M. Gale, Ann. Phys. Fr. **9**, 893 (1984).
[26] J. Chesnoy and G. M. Gale, Adv. Chem. Phys. **70** (part 2), 297 (1988).
[27] T. Elsaesser and W. Kaiser, Annu. Rev. Phys. Chem. **42**, 803 (1991).
[28] J. C. Owrutsky, D. Raftery, and R. M. Hochstrasser, Annu. Rev. Phys. Chem. **45**, 519 (1994).
[29] C. B. Harris, D. E. Smith, and D. J. Russell, Chem. Rev. **90**, 481 (1990).
[30] D. W. Miller and S. A. Adelman, Int. Rev. Phys. Chem. **13**, 359 (1994).
[31] C. Delalande and G. M. Gale, J. Chem. Phys. **71**, 4804 (1979).
[32] W. M. Madigosky and T. A. Litovitz, J. Chem. Phys. **34**, 489 (1961).
[33] P. S. Dardi and R. I. Cukier, J. Chem. Phys. **89**, 4145 (1988).
[34] P. S. Dardi and R. I. Cukier, J. Chem. Phys. **95**, 98 (1991).
[35] B. Khalil-Yahyavi and M. Châtelet, J. Chem. Phys. **92**, 2598 (1990).
[36] B. Oksengorn, Chem. Phys. **140**, 233 (1990).
[37] D. J. Russell and C. B. Harris, Chem. Phys. **183**, 325 (1994).
[38] D. J. Nesbitt and J. T. Hynes, J. Chem. Phys. **77**, 2130 (1982).
[39] R. N. Schwartz, Z. I. Slawsky, and K. F. Herzfeld, J. Chem. Phys. **20**, 1591 (1952).
[40] R. Zwanzig, J. Chem. Phys. **34**, 1931 (1961).
[41] J. K. Brown, C. B. Harris, and J. C. Tully, J. Chem. Phys. **89**, 6687 (1988).
[42] R. M. Whitnell, K. R. Wilson, and J. T. Hynes, J. Phys. Chem. **94**, 8625 (1990).
[43] R. M. Whitnell, K. R. Wilson, and J. T. Hynes, J. Chem. Phys. **96**, 5354 (1992).
[44] I. Benjamin and R. M. Whitnell, Chem. Phys. Lett. **204**, 45 (1993).
[45] R. Rey and J. T. Hynes, J. Chem. Phys. **104**, 2356 (1996).
[46] B. P. Hills, Mol. Phys. **35**, 1471 (1978).
[47] P. S. Dardi and R. I. Cukier, J. Chem. Phys. **86**, 2264 (1987).
[48] P. S. Dardi and R. I. Cukier, J. Chem. Phys. **86**, 6893 (1987).
[49] H. Metiu, D. W. Oxtoby, and K. F. Freed, Phys. Rev. A **15**, 361 (1977).
[50] S. Velsko and D. W. Oxtoby, J. Chem. Phys. **72**, 2260 (1980).
[51] B. Mishra and B. J. Berne, J. Chem. Phys. **103**, 1160 (1995).
[52] J. Chesnoy and J. J. Weis, J. Chem. Phys. **84**, 5378 (1986).
[53] F. E. Figueirido and R. M. Levy, J. Chem. Phys. **97**, 703 (1992).
[54] P. Moore, A. Tokmakoff, T. Keyes, and M. D. Fayer, J. Chem. Phys. **103**, 3325 (1995).
[55] G. Goodyear, R. E. Larsen, and R. M. Stratt, Phys. Rev. Lett. **76**, 243 (1996).
[56] V. M. Kenkre, A. Tokmakoff, and M. D. Fayer, J. Chem. Phys. **101**, 10618 (1994).
[57] D. E. Smith and C. B. Harris, J. Chem. Phys. **92**, 1312 (1990).
[58] M. Tuckerman and B. J. Berne, J. Chem. Phys. **98**, 7301 (1993).
[59] J. S. Bader, B. J. Berne, E. Pollak, and P. Hänggi, J. Chem. Phys. **104**, 1111 (1996).
[60] S. A. Adelman and R. H. Stote, J. Chem. Phys. **88**, 4397 (1988).
[61] R. H. Stote and S. A. Adelman, J. Chem. Phys. **88**, 4415 (1988).

[62] S. A. Adelman, R. Muralidhar, and R. H. Stote, J. Chem. Phys. **95**, 2738 (1991).
[63] J. G. Saven and J. L. Skinner, J. Chem. Phys. **99**, 4391 (1993).
[64] U. Balucani and M. Zoppi, *Dynamics of the Liquid State* (Clarendon, Oxford, 1994).
[65] B. J. Berne and G. D. Harp, Adv. Chem. Phys. **17**, 63 (1970).
[66] J. Hautman and M. L. Klein, Mol. Phys. **80**, 647 (1993).
[67] D. C. Douglass, J. Chem. Phys. **35**, 81 (1961).
[68] D. J. Isbister and D. A. McQuarrie, J. Chem. Phys. **56**, 736 (1972).
[69] G. Zerah and J.-P. Hansen, J. Chem. Phys. **84**, 2336 (1986).
[70] S. A. Egorov, M. D. Stephens, A. Yethiraj, and J. L. Skinner, Mol. Phys. **88**, 477 (1996).
[71] A. Nitzan and R. Silbey, J. Chem. Phys. **60**, 4070 (1974).
[72] J. S. Bader and B. J. Berne, J. Chem. Phys. **100**, 8359 (1994).
[73] K. Tankeshwar, K. N. Pathak, and S. Ranganathan, J. Phys. C **20**, 5749 (1987).
[74] R. M. Stratt and M. Cho, J. Chem. Phys. **100**, 6700 (1994).
[75] I. S. Gradshteyn and I. M. Ryzhik, *Table of Integrals, Series and Products* (Academic, New York, 1965).
[76] J. P. Hansen and I. R. McDonald, *Theory of Simple Liquids*, 2nd ed. (Academic, London, 1986).
[77] J. K. Johnson, J. A. Zollweg, and K. E. Gubbins, Mol. Phys. **78**, 591 (1993).
[78] M. P. Allen and D. J. Tildesley, *Computer Simulation of Liquids* (Clarendon, Oxford, 1987).
[79] J. O. Hirschfelder, C. F. Curtiss, and R. B. Bird, *Molecular Theory of Gases and Liquids* (Wiley, New York, 1954).
[80] G. Herzberg, *Spectra of Diatomic Molecules*, 2nd ed. (Van Nostrand, Toronto, 1950).
[81] R. C. Weast, *Handbook of Chemistry and Physics*, 65th ed. (CRC, Cleveland, 1984).
[82] D. A. McQuarrie, *Statistical Mechanics* (Harper and Row, New York, 1976).